

Coalescence model for Θ_c pentaquark formation *

Marek Karliner

*Cavendish Laboratory, Madingley Road, Cambridge CB3 0HE, U.K.
and*

*School of Physics and Astronomy, Raymond and Beverly Sackler Faculty of Exact Sciences
Tel Aviv University, Tel Aviv, Israel
E-mail: marek@proton.tau.ac.il*

Bryan R. Webber

*Cavendish Laboratory, Madingley Road, Cambridge CB3 0HE, U.K.
E-mail: webber@hep.phy.cam.ac.uk*

ABSTRACT: We present a model for the formation of the charmed pentaquark Θ_c in hard scattering processes such as deep inelastic scattering, e^+e^- annihilation, and high-energy $p\bar{p}$ collisions. The model assumes that the cross section for Θ_c formation is proportional to the rate of production of pD^{*-} (or $\bar{p}D^{*+}$) pairs in close proximity both in momentum space and in coordinate space. The constant of proportionality is determined from the Θ_c cross section in deep inelastic scattering as reported by the H1 experiment. The HERWIG Monte Carlo is used to generate simulated DIS events and also to model the space-time structure of the final state. Requiring the proton and the D^* be within a 100 MeV mass window and separated by a spacelike distance of no more than 2 fm, we find that a large “coalescence enhancement factor” $F_{co} \sim 10$ is required to account for the H1 signal. The same approach is then applied in order to estimate the number and characteristics of Θ_c events produced at LEP and the Tevatron.

KEYWORDS: QCD, Phenomenological Models, Deep Inelastic Scattering.

*Work supported in part by the UK Particle Physics and Astronomy Research Council and by the Royal Society.

Contents

1. Introduction	1
2. Coalescence model	2
2.1 Model for space-time structure	3
2.2 DIS results	3
2.3 e^+e^- results	9
2.4 Hadroproduction results	14
3. Summary and conclusions	16

1. Introduction

During the last year, many experiments have reported the observation of an exotic $uudd\bar{s}$ pentaquark baryon Θ^+ [1, 2]. Shortly after the initial experimental reports, Ref. [3] postulated the existence of an anti-charmed analogue Θ_c with quark content $uudd\bar{c}$, and computed its likely properties, using the diquark-triquark configuration earlier conjectured to describe Θ^+ [4].

Ref. [3] suggested that Θ_c is an isosinglet with $J^P = \frac{1}{2}^+$ and estimated its mass at 2985 ± 50 MeV. It also discussed another possible exotic baryon resonance containing heavy quarks, the Θ_b^+ , a $uudd\bar{b}$ state, and estimated $M(\Theta_b^+) = 6398 \pm 50$ MeV, noting that these states should appear as unexpectedly narrow peaks in D^-p , \bar{D}^0n , B^0p and B^+n mass distributions. Possible search opportunities in e^+e^- have also been suggested in Refs. [5, 6, 7].

In March, H1 reported [8] observing a narrow resonance in $D^{*-}p$ and $D^{*+}\bar{p}$ invariant mass combinations in inelastic ep collisions at E_{CM} of 300 GeV and 320 GeV at HERA. The resonance has a mass of 3099 ± 3 (stat.) ± 5 (syst.) MeV and a measured Gaussian width of 12 ± 3 (stat.) MeV, compatible with the experimental resolution. The experiment interpreted this resonance as an anti-charmed baryon with a minimal constituent quark composition of $uudd\bar{c}$, together with the charge conjugate.

A parallel analysis by ZEUS sees no signal [9]. Null results have also been reported in papers and unpublished reports at conferences by FOCUS [10], ALEPH [11] and CDF [12].

Since H1 observes the resonance in both $D^{*-}p$ and $D^{*+}\bar{p}$, it is extremely unlikely that their result is due to a statistical fluctuation.

Since the ZEUS and H1 experiments are quite similar, a possible interpretation of these results is that Θ_c does not exist and the H1 observation is due to some yet to

be understood systematic effect. The discrepancy between H1 and ZEUS is of a purely experimental nature. It is now being carefully examined by the two collaborations.

Putting the ZEUS vs H1 issue aside for the time being, an important question is: what are the implications of the null results in non-HERA experiments? Since production mechanisms might be different in different experiments, an *a priori* possible interpretation is that these experiments have not accumulated enough data or that more sophisticated cuts need to be applied in order to separate the likely small Θ_c signal from the background. In the present paper we examine the quantitative implications of a possible H1-like production mechanism at LEP and the Tevatron.

One can try to apply a simple counting argument to the H1 data in order to estimate the expected number of events at LEP. The H1 data sample of 75 pb^{-1} of DIS events contains roughly 1.5×10^6 events with charm. This should be compared with the corresponding numbers for Z^0 decays at LEP:

$$\begin{aligned}\Gamma(\text{hadrons})/\Gamma_{\text{total}} &= 0.70, \\ \Gamma(c\bar{c})/\Gamma(\text{hadrons}) &= 0.17,\end{aligned}\tag{1.1}$$

so $\Gamma(c\bar{c})/\Gamma_{\text{total}} = 0.12$. After cuts, each of the LEP experiments has several million hadronic Z^0 decays. Specifically, ALEPH [11] has 3.5×10^6 , corresponding to approximately 6×10^5 charm events.

We can use this number to make a very crude estimate of the number of expected anticharm pentaquark events at LEP. If the production mechanisms at H1 and LEP are roughly similar, the expected number of anticharmed pentaquarks events at each of the four LEP experiments is about 40% of the number of such events at H1.

In the rest of the paper we carry out this estimate in more detail, with a coalescence model providing a specific possible mechanism for Θ_c formation from D^*p , and HERWIG generating the corresponding D^* and p distributions.

The result of this analysis is that each of the LEP experiments should have observed between 25 and 40 charmed pentaquark events of the H1 type. This takes into account typical experimental cuts and efficiencies.

At the Tevatron, the integrated luminosity already collected in Run II is of the order of 200 pb^{-1} . If the production mechanism is the same as in H1, we conclude that even with a very low overall detection efficiency of only a few per mille, this would provide an unmissable signal on the order of 10^5 events.

In the following sections of the paper we develop the model, extract the relevant coalescence parameter from the H1 data and then apply it to LEP and Tevatron experiments. We then discuss several possible interpretations of these results.

2. Coalescence model

We construct a simple but, we believe, physically appealing model to attempt a quantitative estimate of the expected production rate of Θ_c via coalescence of a D^* and a nucleon. We use the Monte Carlo program HERWIG [13, 14] to generate simulated DIS events with

HERA kinematics, selecting those which include either p and D^{*-} or \bar{p} and D^{*+} . In addition to the momentum-space structure of final states, HERWIG generates an approximate space-time structure, which enables us to model the joint distribution of invariant mass and space-time separation of the pD^* pairs. Assuming resonance formation through coalescence, we suppose that the cross section for Θ_c production is proportional to the number of pD^* pairs that have invariant masses in a small interval Δm around the resonance mass and are at the same time formed within a small spacelike separation Δx . By adjusting the constant of proportionality to match the Θ_c signal observed in DIS by H1, we predict the Θ_c signal that should be seen in other processes with a similar production mechanism.

2.1 Model for space-time structure

Since the space-time structure of the final state is a crucial ingredient of the proposed coalescence mechanism, we start with a brief summary of the HERWIG model for this structure. Fuller details may be found in ref. [13].

During development of the final state, HERWIG assigns to each unstable object with four-momentum q an exponentially distributed proper lifetime, with mean value τ given by [15]

$$\tau = \frac{\hbar\sqrt{q^2}}{\sqrt{(q^2 - M^2)^2 + (\Gamma q^2/M)^2}} \quad (2.1)$$

where M and Γ are the nominal mass and width. This formula interpolates between $\tau = \hbar/\Gamma$ for an object that is on mass-shell and $\tau = \hbar\sqrt{q^2}/(q^2 - M^2)$ for one that is far off mass-shell. Following sequential electroweak decays and QCD parton showers, the resulting space-time separations are combined to give the locations of partons at the start of the hadronization process.

For light quarks and gluons, whose natural widths are small, the above prescription can lead to unreasonably large distances being generated in the final, low-virtuality steps of parton showering. To avoid this they are given a width $\Gamma = \text{VMIN2}/M$, the HERWIG parameter `VMIN2` (default value 0.1 GeV²) acting as a lower limit on a parton's virtuality.

Hadronization in HERWIG takes place through non-perturbative gluon splitting, $g \rightarrow q\bar{q}$, followed by colour-singlet $q\bar{q}$ cluster formation and decay. The production vertex of a cluster is taken as the midpoint of a line perpendicular to the cluster's direction of travel, with its two ends on the trajectories of the constituent quark and antiquark. The production positions of primary hadrons from cluster decays are smeared, relative to the cluster position, according to a Gaussian distribution of width \hbar/M where M is the mass of the cluster.

2.2 DIS results

We first use HERWIG to simulate DIS in e^+p collisions with beam momenta 27.6×920 GeV/c and integrated luminosity 75 pb^{-1} , which approximates the data sample used in the H1 analysis [8]. For greater efficiency, we limit the target partons to charmed quarks and antiquarks only, by setting the process code `IPROC` = 9004. Using the HERWIG default (MRST LO [16]) parton distribution functions, we find a total leading-order DIS-on-charm

cross section of 18.4 nb for momentum transfers in the region $6 < Q^2 < 100$ GeV 2 and inelasticities $0.05 < y < 0.7$. We therefore generate 1.4×10^6 simulated events so as to correspond roughly to the 75 pb^{-1} integrated luminosity of the H1 data sample. In HERWIG runs with $\text{IPROC} = 9000$ (DIS on all flavours of partons), we find that the contribution to pD^* production in the region of interest from DIS on non-charmed partons is negligible.

We use a momentum transfer range of $6 < Q^2 < 100$ GeV 2 , rather than the full range $1 < Q^2 < 100$ GeV 2 covered by the H1 analysis, because the charm PDF and HERWIG simulation are not reliable at lower Q^2 . The predicted dependence of the $D^{*\pm}$ cross section on Q^2 is shown in fig. 1 together with the recent H1 data [17]. The predicted D^* pseudorapidity distribution is shown with the H1 data in fig. 2. These results can also be compared with ZEUS results [18] for charm production in DIS.

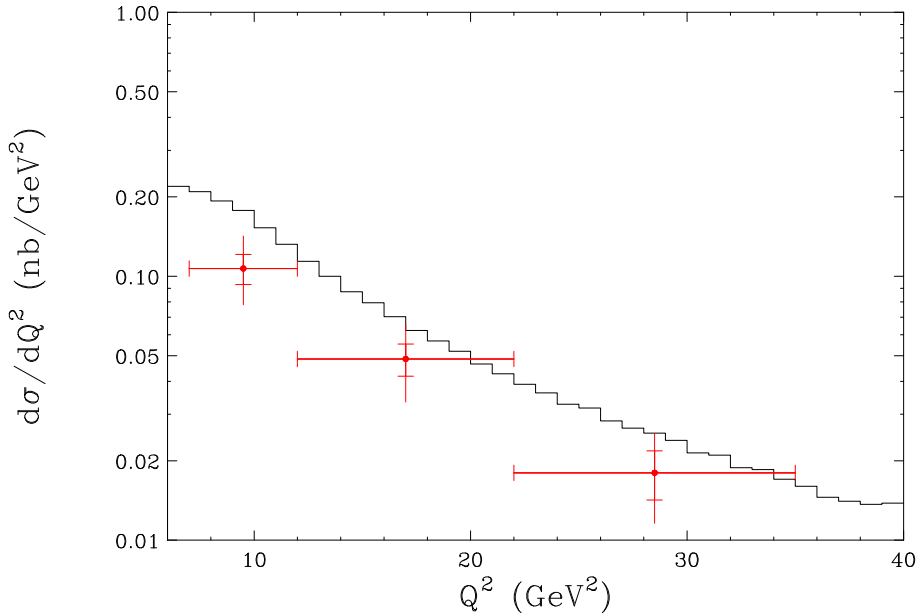


Figure 1: HERWIG prediction for $D^{*\pm}$ production in DIS at $Q^2 > 6$ GeV 2 , together with recent H1 data [17].

The histograms in figs. 1 and 2 are for the cuts in ref. [8], while the data shown are for slightly different cuts (see ref. [17] for details), which we estimate may reduce the cross section by 30-40% without changing the shape significantly. In view of the more limited range of Q^2 accessible in the HERWIG simulation, a detailed comparison with the data is not possible at present, but we judge the semi-quantitative agreement to be satisfactory.

Next we select events in which both a proton and a D^{*-} , or an antiproton and a D^{*+} , are produced. Imposing the cuts in Table 1, which approximate those applied in the H1 analysis, but not yet selecting particular D^* decays, we obtain the pD^* mass spectrum shown by the solid histogram in fig. 3.

$p_t(p)_{\min}$	120 MeV
$p_t(D^*)_{\min}$	1.5 GeV
$\eta(D^*)_{\min}$	-1.5
$\eta(D^*)_{\max}$	1.0
$z(D^*)_{\min}$	0.2

Table 1: Selection criteria for pD^* production.

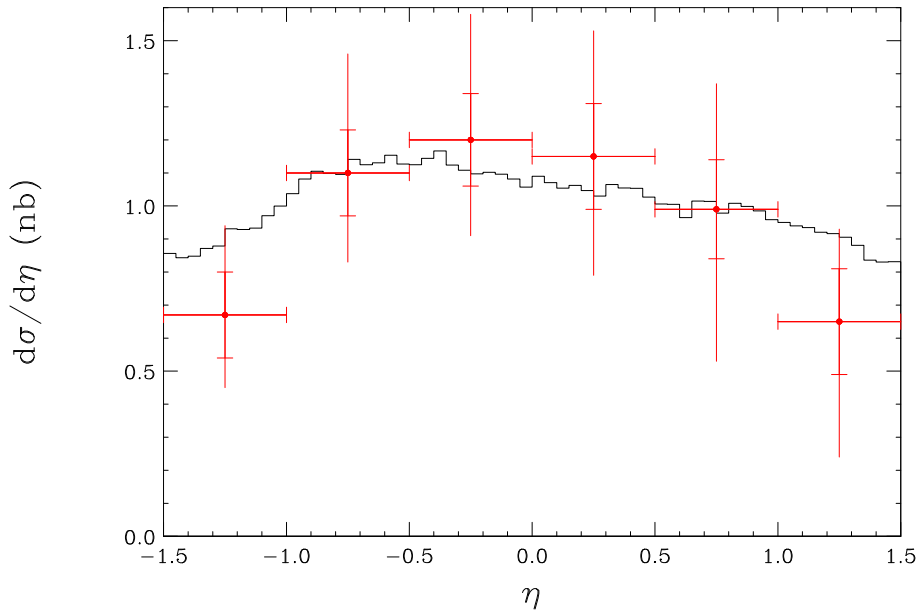


Figure 2: Predicted $D^{*\pm}$ pseudorapidity distribution in DIS, together with recent H1 data [17].

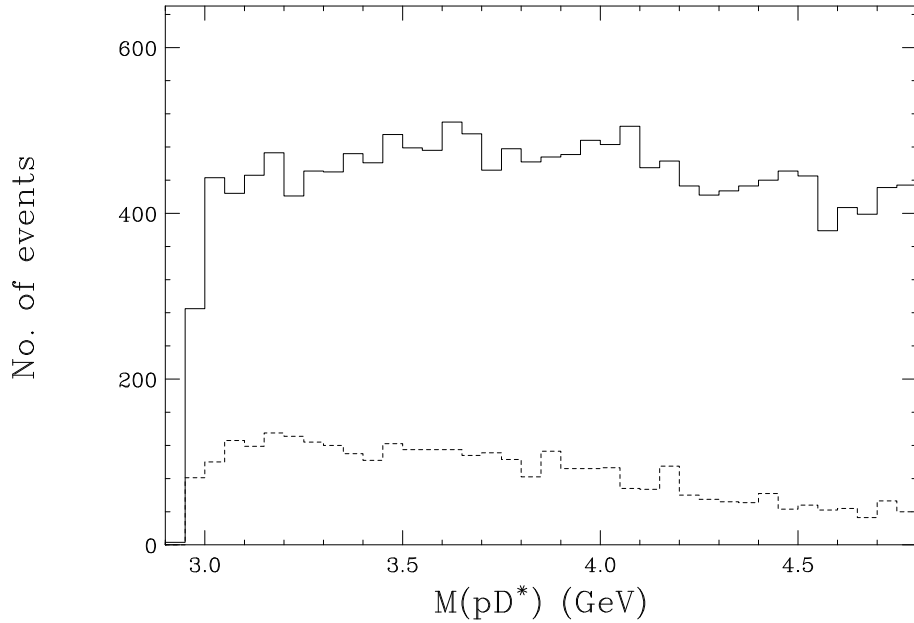


Figure 3: Predicted non-resonant pD^* mass distribution in DIS. Solid: all pD^{*-} and $\bar{p}D^{*+}$ pairs. Dashed: pairs with separation $0 < \Delta x < 2$ fm.

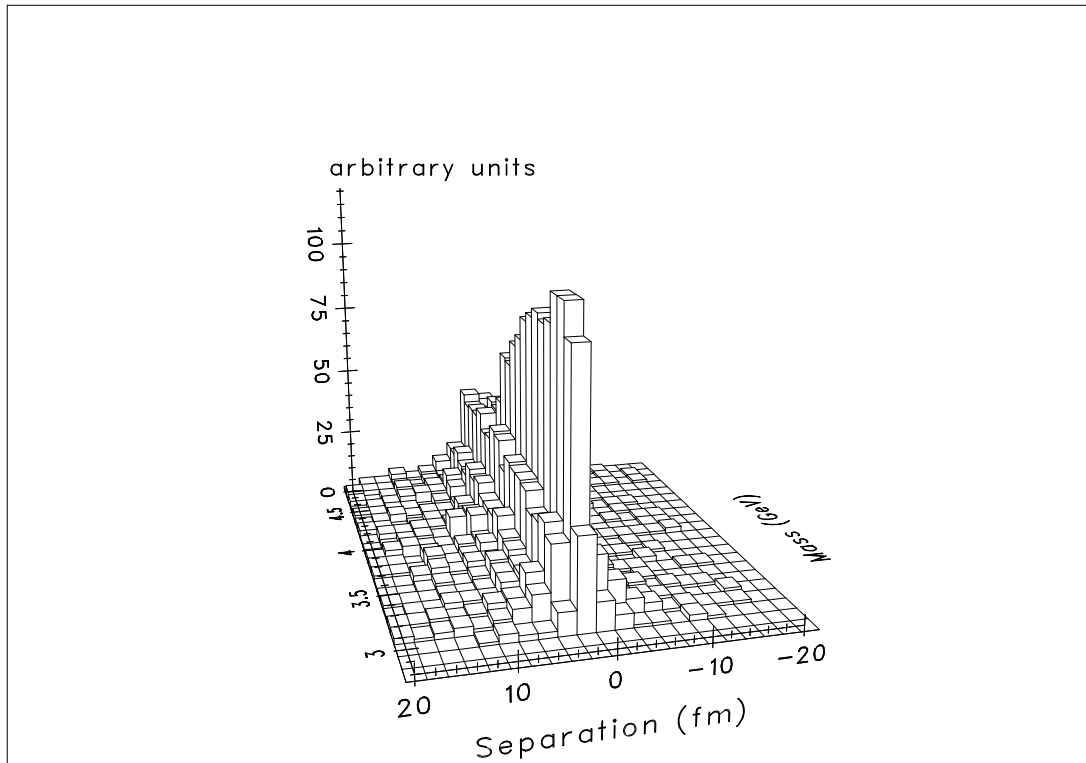


Figure 4: Predicted pD^* joint mass–separation distribution in DIS.

The predicted joint distribution in mass and space-time separation is shown in fig. 4. Here we depict spacelike separations as positive and timelike as negative. There is a preference for spacelike separations, peaking at small values, corresponding to the formation of primary hadrons on a hyperboloid at a roughly universal proper hadronization time. This should be a general characteristic of physically reasonable hadronization models.

We now suppose that the Θ_c resonance, not explicitly present in the HERWIG hadronization scheme, can be modelled as an enhancement in the cross section proportional to the number of pD^* pairs with invariant masses in a window Δm close to resonance and at the same time within the range Δx of the binding mechanism. The measures of closeness should be on the hadronic scale of $\Delta m \sim 100$ MeV, $\Delta x \sim 1$ fm. To be specific, we choose the mass interval $3050 < m < 3150$ MeV and spacelike separations $0 < \Delta x < 2$ fm.

The predicted mass distribution for pD^* pairs with separations $0 < \Delta x < 2$ fm is shown by the dashed histogram in fig. 3. Of these pairs, 245 fall within the coalescence region $3050 < m < 3150$ MeV. With a coalescence enhancement factor F_{co} , we therefore expect of the order of $250F_{\text{co}}$ events with Θ_c production.

In the H1 experiment, the $D^{*\pm}$ is detected through the decay sequence $D^{*\pm} \rightarrow D^0\pi^\pm$, $D^0 \rightarrow K^-\pi^+$, which has a branching fraction of about 3%. Taking into account the H1 cuts needed to identify the decay products, listed in Table 2, we estimate that this fraction is reduced to roughly 2%. Therefore the expected H1 Θ_c signal is about $5F_{\text{co}}$ events. Given the observed signal of 50 events, this implies a rather large coalescence enhancement factor of $F_{\text{co}} \simeq 10$.

To obtain the observed pD^* mass distribution from the one shown by the solid histogram in fig. 3, one should multiply by the $D^{*\pm}$ detection efficiency. The shape of the distribution is similar to that shown in ref. [8], but the above efficiency estimate of 2% implies an observed number of about 10 pairs per 50 MeV bin, which is considerably smaller than the number of about 10 pairs per 10 MeV bin found by H1. This could be due to an underestimate of the proton yield by HERWIG, a higher relative proton yield in charm production with $1 < Q^2 < 6 \text{ GeV}^2$, or a large contamination of the experimentally reported distribution by non-protons.

We expect the predicted proton yield in the coalescence region to be more reliable, since additional soft contributions will tend to be more widely distributed in space-time. We therefore use the value $F_{\text{co}} \simeq 10$ throughout the rest of this paper. However, it should be borne in mind that an enhancement of the proton density in the coalescence region in DIS would imply a reduced value of the coalescence factor F_{co} and hence a smaller prediction of Θ_c production in other processes. On the basis of the information available to us, we estimate the maximal range of values indicated by the H1 signal to be $2 \lesssim F_{\text{co}} \lesssim 10$.

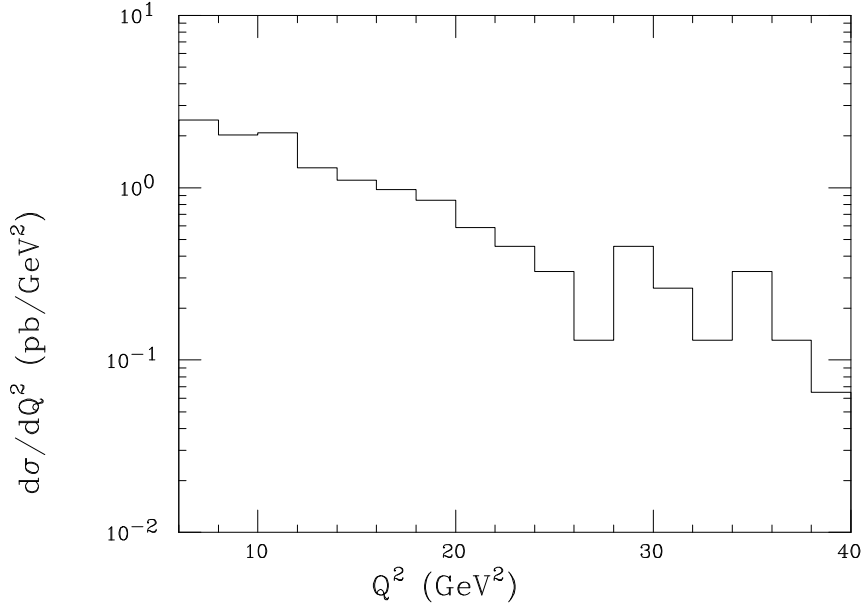


Figure 5: Predicted Θ_c production cross section as a function of momentum transfer in DIS.

Of course, changing the size of the coalescence region by varying Δm and/or Δx can be compensated by a change in F_{co} to give the same signal. For example, one could increase the mass interval to 200 MeV, i.e. $3000 < m < 3200$ MeV, and the maximum separation to 4 fm. Then a value of $F_{\text{co}} \simeq 2.5$ would account for the H1 signal, without changing substantially the predictions given below. This stability against variation of Δm and/or Δx provides a nontrivial test of the coalescence model's robustness.

Having fixed the coalescence factor F_{co} , we can make predictions about other aspects of Θ_c production in DIS. For example, we show in fig. 5 the predicted Θ_c production cross section in DIS as a function of the momentum transfer Q^2 . The rather weak dependence at low Q^2 helps to justify our exclusion of the region $Q^2 < 6 \text{ GeV}^2$. Figures 6 and 7 show the predicted pseudorapidity and transverse momentum distributions of the Θ_c , computed from the corresponding quantities for pD^* pairs in the coalescence region.

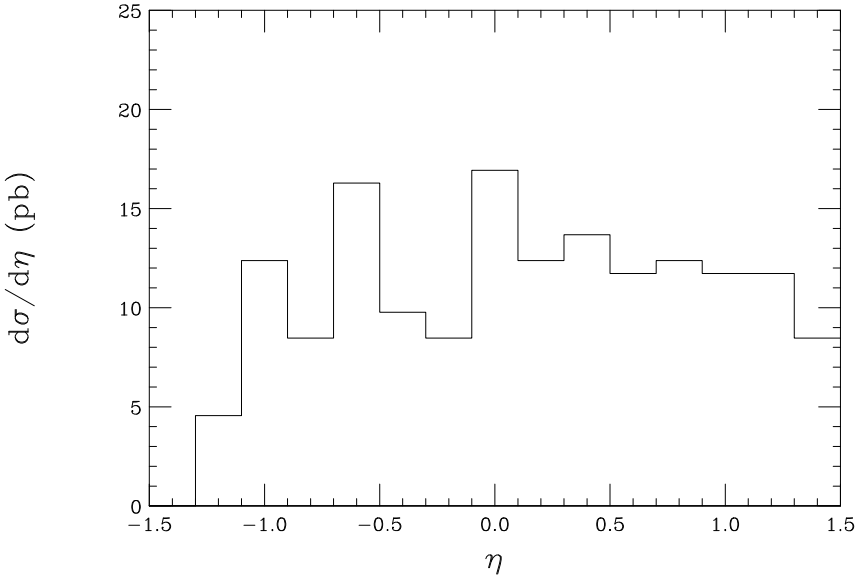


Figure 6: Predicted Θ_c pseudorapidity distribution in DIS.

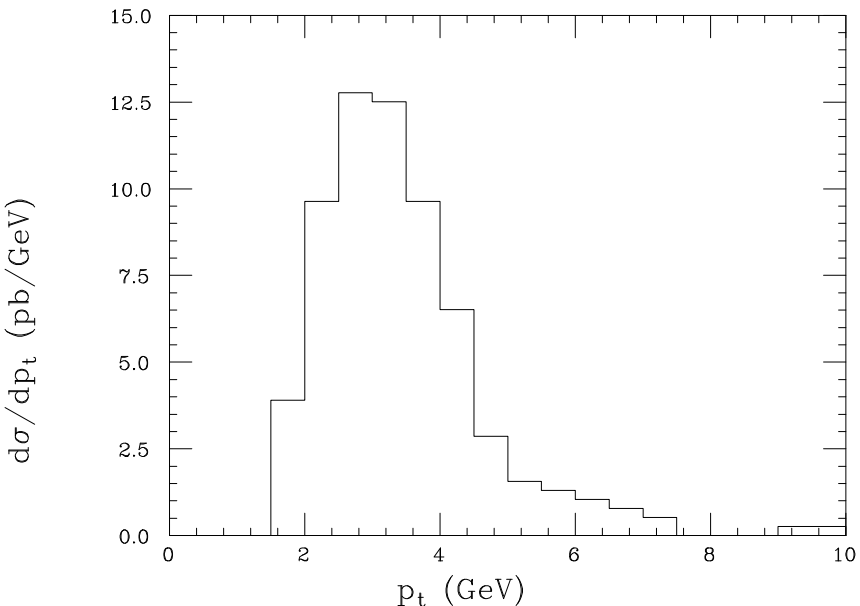


Figure 7: Predicted Θ_c transverse momentum distribution in DIS.

2.3 e^+e^- results

The coalescence model can be used to predict the rates and distributions of Θ_c production in other hard processes that can be generated by HERWIG, such as e^+e^- annihilation. We simply assume that the Θ_c distributions are always in the fixed ratio $F_{co} = 10$ to those of pD^* pairs in the coalescence region of Δm and Δx .

We concentrate on the resonant reaction $e^+e^- \rightarrow Z^0 \rightarrow$ hadrons since this is the place where the LEP experiments accumulated most of the data that might show evidence of Θ_c production. We generate 7×10^5 simulated events of the process $e^+e^- \rightarrow Z^0 \rightarrow c\bar{c}$ at the resonance peak, which corresponds to the approximate integrated luminosity of 140 pb^{-1} collected by each experiment at or near Z^0 resonance. Although the process $e^+e^- \rightarrow Z^0 \rightarrow b\bar{b}$ is a copious indirect source of charm, the possible production of Θ_c in b -decay is a separate issue and we assume that this source could be distinguished experimentally from direct production. As in the case of DIS, we find that, within the framework of the HERWIG model, the contribution to pD^* production in the coalescence region from light quark production ($e^+e^- \rightarrow Z^0 \rightarrow q\bar{q}$ where $q = u, d, s$) is negligible.

We apply no selection criteria like those in Tables 1 and 2, since these are mostly irrelevant to the LEP environment. Therefore our predictions represent upper limits on the observable signal at LEP1 for consistency with the H1 data and the coalescence model.

Figure 8 shows the resulting pD^* joint distribution in mass and space-time separation, to be compared with fig. 4 for DIS. The two distributions are similar, with some additional narrowing of the mass distribution at small separations in the case of Z^0 decay.

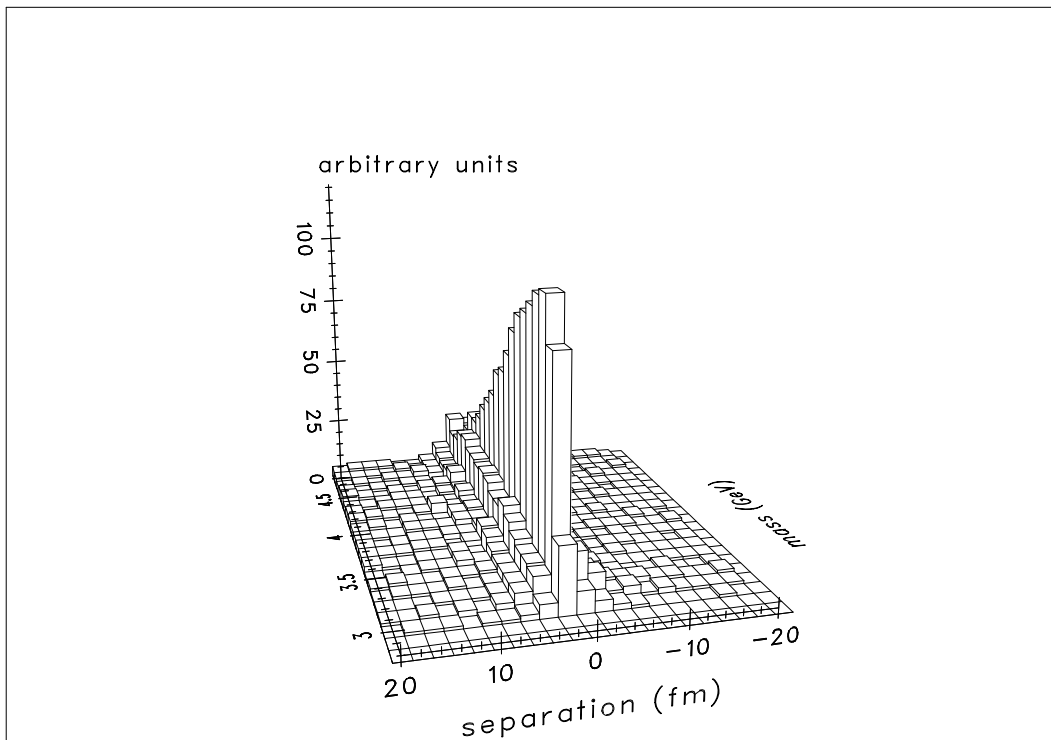


Figure 8: Predicted pD^* joint mass–separation distribution in Z^0 decay.

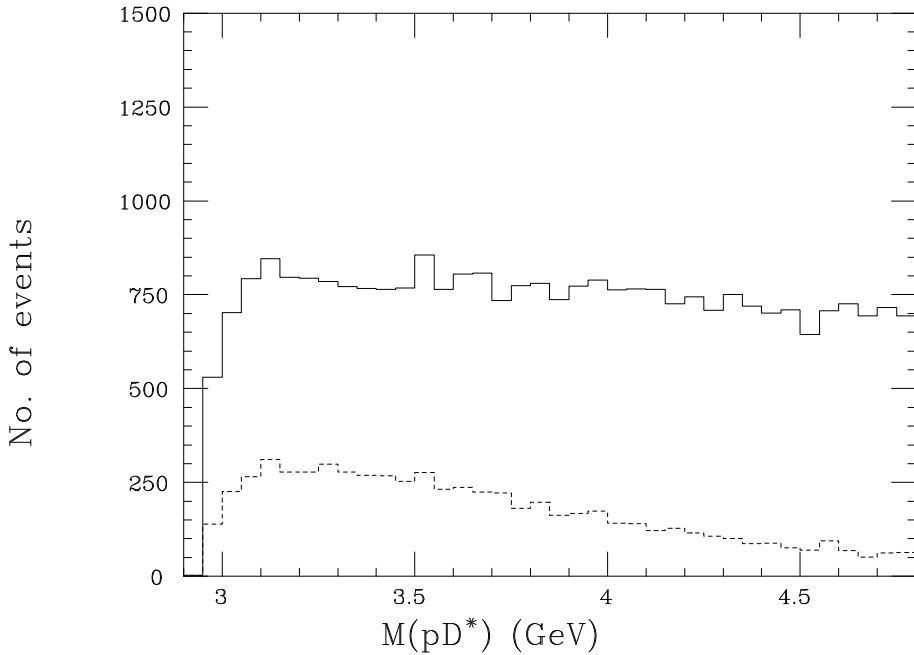


Figure 9: Predicted non-resonant pD^* mass distribution in Z^0 decay. Solid: all pD^{*-} and $\bar{p}D^{*+}$ pairs. Dashed: pairs with separation $0 < \Delta x < 2$ fm.

The overall pD^* mass distribution is shown by the solid histogram in fig. 9, corresponding to fig. 3 for DIS. In order to make a comparison with experiment, we need to take into account data reduction due to cuts and efficiencies. We generated 7×10^5 charm events, corresponding to $7 \times 10^5 / 0.17 = 4.1 \times 10^6$ hadronic events, to be compared with 3.5×10^6 hadronic events reported by ALEPH [11] after cuts. ALEPH reports 1.3M proton candidates, whereas the proton yield is about 1 per event, so their mean proton efficiency is $\sim 1/3$. For the D^* efficiency, through $D^{*\pm} \rightarrow D^0\pi^\pm$, $D^0 \rightarrow K^-\pi^+$, we assume a range 2-3%. These cut and efficiencies yield a reduction factor between 5.7×10^{-3} and 8.5×10^{-3} .

In [11] ALEPH reports 82 $D^{*-}p$ events in the mass range $2.95 \text{ GeV} < M(D^{*-}p) < 4 \text{ GeV}$. The total number of $D^{*-}p$ events in this mass range in fig. 9 is about 15,000, so we would expect between 85 and 130 events to be seen, in good agreement with [11].

The mass distribution after a cut on separation is shown by the dashed histogram in fig. 9. The number of pairs in the coalescence region $0 < \Delta x < 2$ fm, $3050 < m < 3150$ MeV is 576, roughly as expected from the 245 found in DIS with about half the integrated luminosity. The corresponding Θ_c production cross section on resonance, assuming a coalescence enhancement factor of $F_{\text{co}} \simeq 10$, is 40 pb. Taking into account the data reduction factors above, that implies a signal of about 25-40 events per experiment in the observed decay channel.

The predicted distribution of Θ_c production with respect to the momentum fraction $x_p = 2|\mathbf{p}|/\sqrt{s}$ is shown in fig. 10. This distribution is similar in shape to that of the $D^{*\pm}$, but slightly narrower (fig. 11). The predicted Θ_c production is strongly collimated along the jet axes of the final state, as shown by the pseudorapidity and transverse momentum distributions relative to the thrust axis (figs. 12, 13).

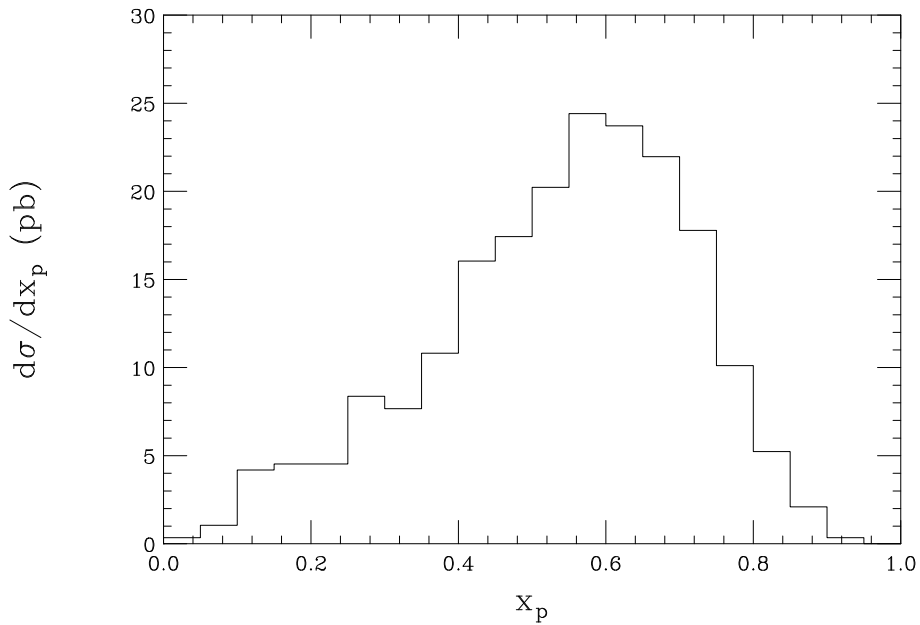


Figure 10: Predicted cross section $e^+e^- \rightarrow Z^0 \rightarrow \Theta_c X$ as a function of momentum fraction.

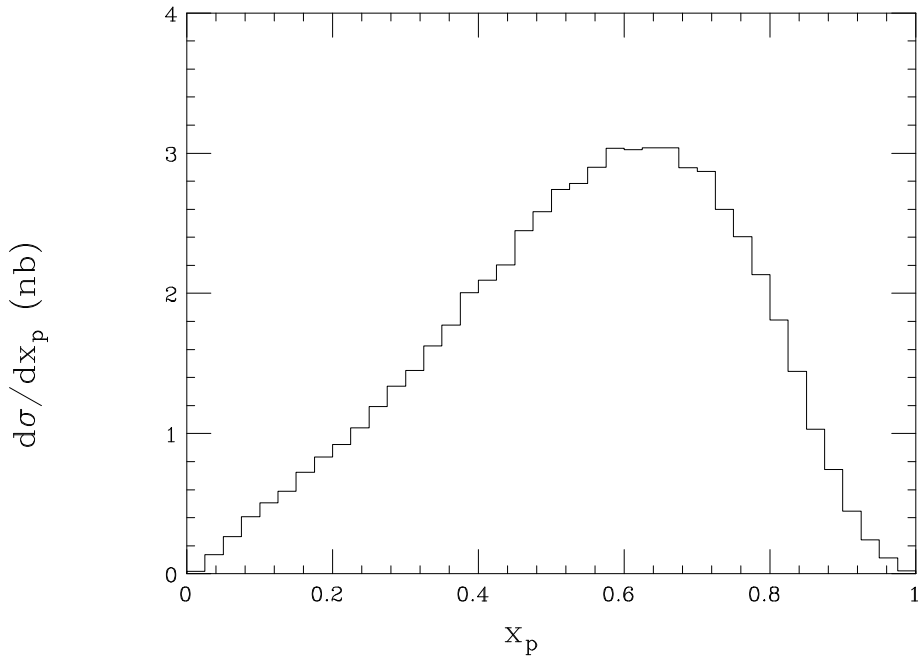


Figure 11: Predicted cross section $e^+e^- \rightarrow Z^0 \rightarrow D^{*\pm} X$ as a function of momentum fraction.

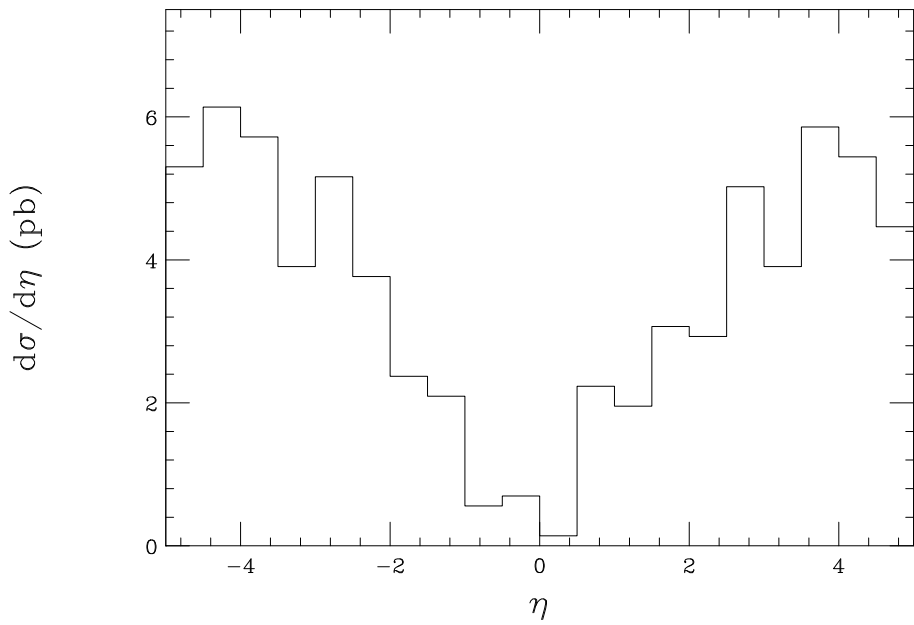


Figure 12: Predicted cross section $e^+e^- \rightarrow Z^0 \rightarrow \Theta_c X$ as a function of pseudorapidity relative to the thrust axis.

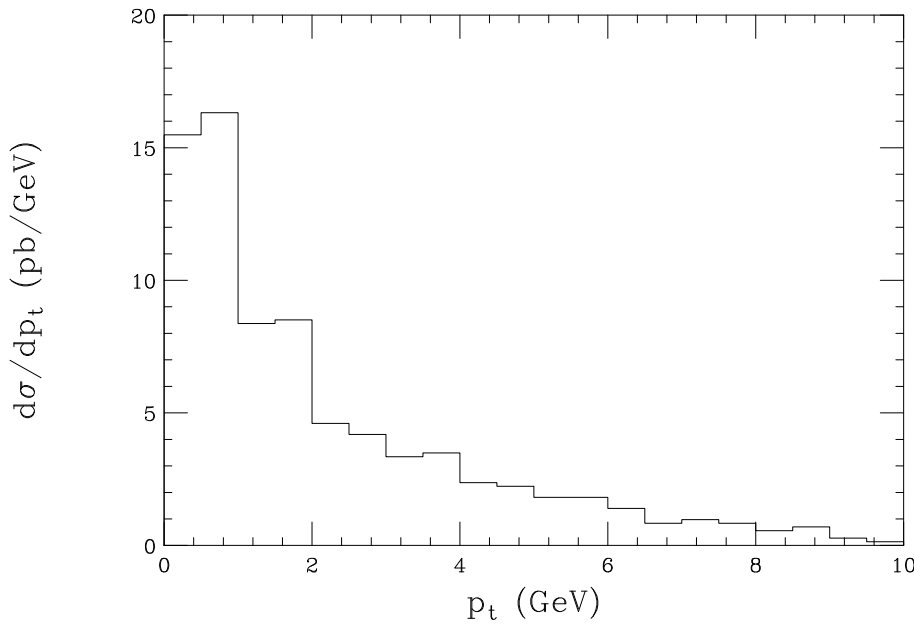


Figure 13: Predicted cross section $e^+e^- \rightarrow Z^0 \rightarrow \Theta_c X$ as a function of transverse momentum relative to the thrust axis.

In contrast, ALEPH reports [11] no deviation from background in the relevant mass region, i.e. no signal. Our results then have several possible interpretations:

- (a) there is no resonance and the H1 signal is due to some yet to be understood systematic effect;
- (b) H1 observed a genuine resonance, but for some reason the production mechanism in DIS is different than in e^+e^- ;
- (c) the production mechanism is the same in DIS and e^+e^- but it is not described by the coalescence model;
- (d) some crucial ingredient in the e^+e^- data analysis is not well understood.

In this context we would like to draw the reader's attention to two examples of non-exotic baryon states which are definitely known to exist, but whose study seems to be problematic at LEP.

The first example is $\Lambda_c(2880)^+$ which is above the ND threshold. According to RPP [19], the only observed decay modes of $\Lambda_c(2880)^+$ are $\Lambda_c^+\pi^+\pi^-$ and $\Sigma_c(2550)\pi$. So is unclear why no one has seen $\Lambda_c(2880)^+ \rightarrow DN$ (D^*N is above threshold).

An even more striking example is the non-observation of (anti)-deuterons at LEP. As already noted elsewhere [20], it is also useful to compare the rate of antideuteron and antiproton production in a given experiment. Such an analysis has been carried out by H1 [21], yielding an antideuteron/antiproton ratio of $\bar{d}/\bar{p} = 5.0 \pm 1.0 \pm 0.5 \times 10^{-4}$ in photoproduction.

On the other hand, although the LEP experiments produced roughly one proton per Z^0 decay [22] and have accumulated millions of Z^0 decays on tape, very little is known about antideuteron production at LEP. The one theoretical prediction we are aware of is Ref. [23], which uses the Lund string fragmentation model to predict 5×10^{-5} deuterons per Z^0 decay. The only relevant experimental publication we are aware of is from OPAL [24], which reports exactly *one* antideuteron candidate event which was eventually dismissed because it did not pass through the primary vertex. From this OPAL infers at 90% confidence level an upper limit on antideuteron production of 0.8×10^{-5} antideuterons per Z^0 in the momentum range $0.35 < p < 1.1$ GeV.

A recent estimate [25] based on this data concludes that $\bar{d}/\bar{p} < 1.6 \times 10^{-4}$, which is significantly less than the ratio reported by H1 [21].¹ The reason for this presumed difference is unknown at present. In analogy with Θ_c formation, one can construct a coalescence model for deuteron formation. Using a similar coalescence window ($m - m_p - m_n < 100$ MeV, $0 < \Delta x < 2$ fm), the LEP upper limit implies a coalescence factor for $\bar{p} + \bar{n} \rightarrow \bar{d}$, of $F_{\text{co}}^{(d)} < 0.1$. It would be very valuable to have more information on antideuterons from the LEP experiments.

¹We thank T. Sloan for discussion of this point.

2.4 Hadroproduction results

The Θ_c coalescence model can also be used to predict its production in hadron-hadron collisions. The only limitation, as in DIS, is that HERWIG is able to model only hard processes. In heavy quark hadroproduction the quark mass provides a hard scale, but in the case of charm this is not large enough to ensure perturbative reliability. We therefore set a minimum transverse momentum for the hard subprocess, setting the HERWIG parameter `PTMIN` to 5 GeV. This means that charmed hadron production can only be predicted at transverse momenta greater than this value.

The prediction for $D^{*\pm}$ production above 5 GeV in Tevatron Run II ($p\bar{p}$ at $\sqrt{S} = 2$ TeV), shown in fig. 14, is indeed in reasonable agreement with CDF preliminary data [26].

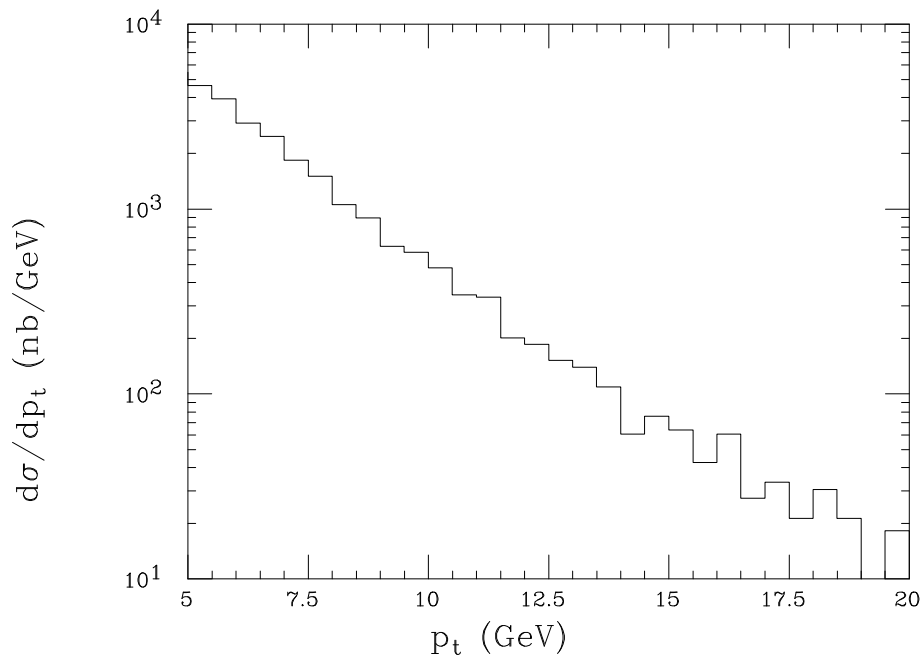


Figure 14: HERWIG prediction for $D^{*\pm}$ transverse momentum distribution in $p\bar{p}$ collisions at $\sqrt{S} = 2$ TeV.

The model study presented here is based on a sample of 10^5 simulated charm production events. The HERWIG estimate of the charm cross section with the above transverse momentum cut is 0.15 mb. Therefore the equivalent integrated luminosity of our sample is quite small, around 0.7 nb^{-1} .

Figure 15 shows the corresponding pD^* joint distribution in mass and space-time separation, to be compared with figs. 4 and 8 for DIS and Z^0 decay, respectively. We see that the distribution in hadroproduction is substantially broader in both variables. This is due to the more complex structure of hadron-hadron collisions. In particular, the underlying event (due to interactions between the beam hadron remnants) often contains protons and antiprotons formed over a longer timescale than that required for coalescence.

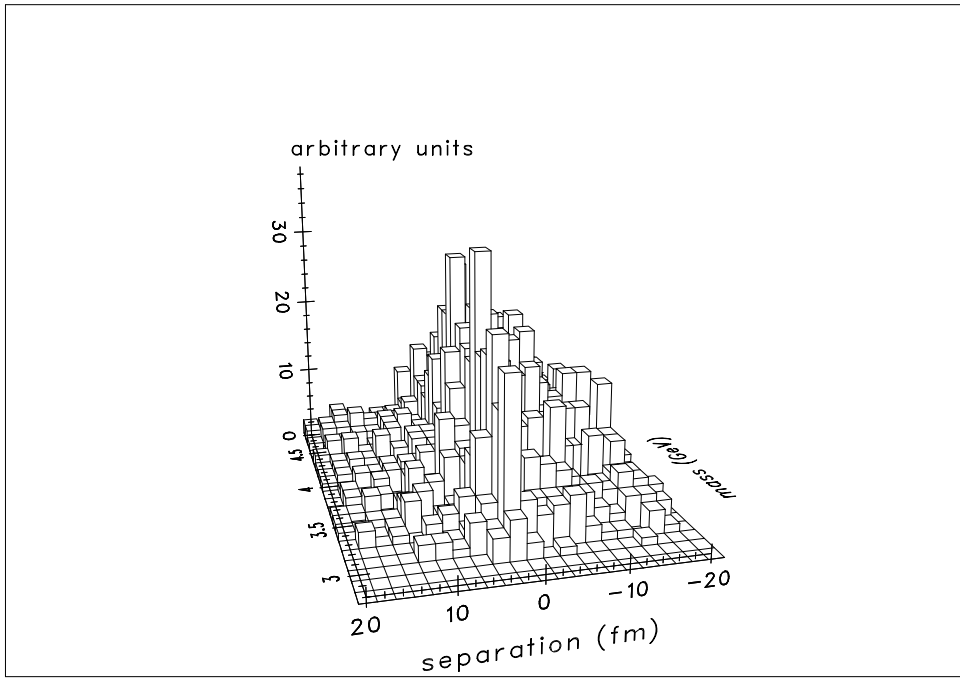


Figure 15: Predicted pD^* joint mass–separation distribution in charm hadroproduction at $\sqrt{S} = 2$ TeV.

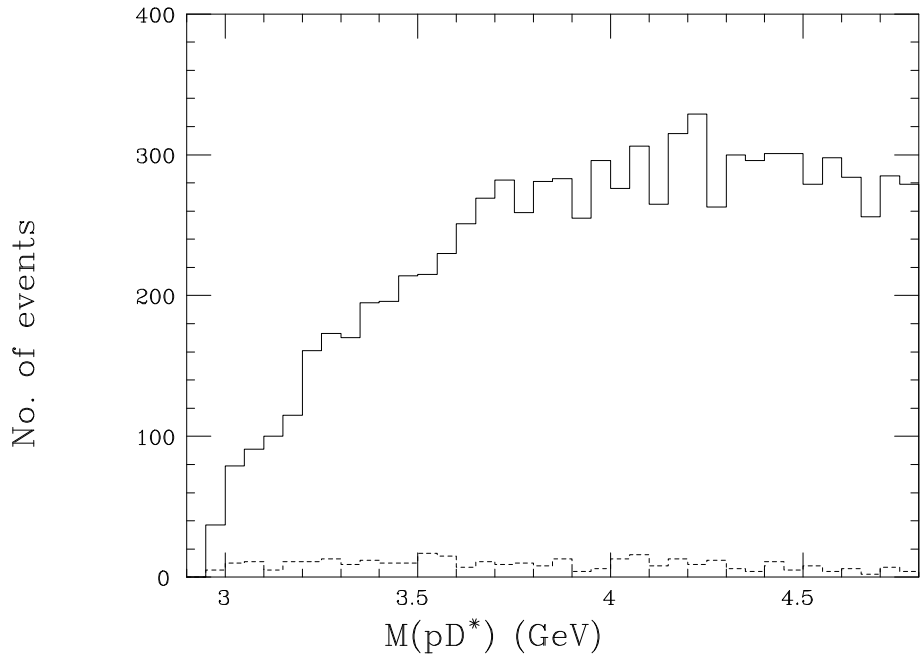


Figure 16: Predicted non-resonant pD^* mass distribution in charm hadroproduction at $\sqrt{S} = 2$ TeV. Solid: all pD^{*-} and $\bar{p}D^{*+}$ pairs. Dashed: pairs with separation $0 < \Delta x < 2$ fm.

The pD^* mass distributions before and after a cut on separation are shown in fig. 16, corresponding to figs. 3 and 9. The predicted Θ_c transverse momentum distribution is shown in fig. 17. The number of pairs in the coalescence region $0 < \Delta x < 2$ fm, $3050 < m < 3150$ MeV is 16. Taking into account coalescence factor $F_{\text{co}} \simeq 10$, this corresponds to 160 Θ_c events, i.e. to a Θ_c production cross section of 240 nb. Since the integrated luminosity already collected in Run II is of the order of 200 pb^{-1} , this corresponds to production of some 50 million Θ_c 's. Even with an overall detection efficiency of only a few per mille, this would seem to provide an unmissable signal.

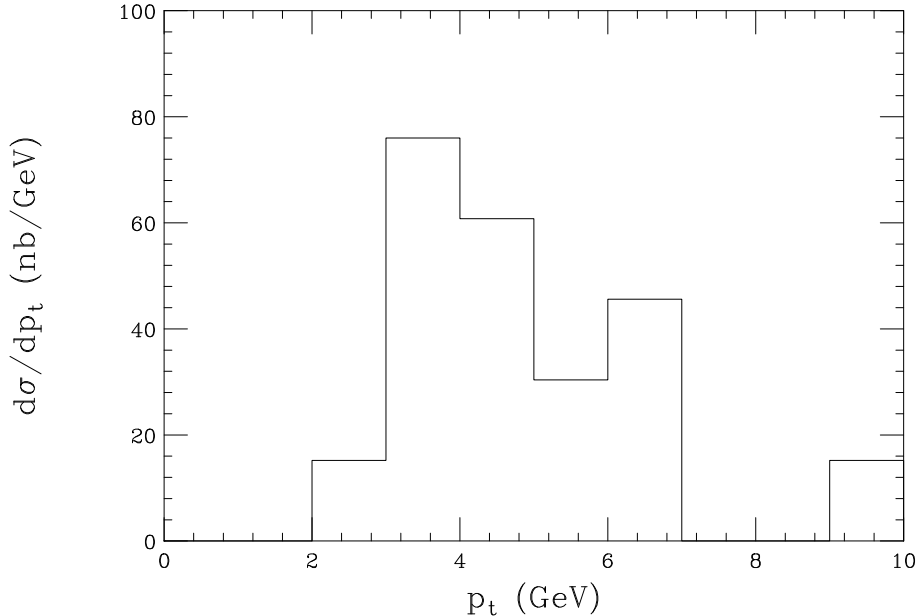


Figure 17: Predicted Θ_c transverse momentum distribution in $p\bar{p}$ collisions at $\sqrt{S} = 2$ TeV.

3. Summary and conclusions

We constructed a simple coalescence model for the production of the charmed pentaquark reported by the H1 experiment. This model can also serve as a template for estimating resonance and bound state production cross sections in a wide range of hard processes.

In the specific case discussed here pentaquark formation is assumed to occur when D^*p are in close proximity in both momentum and coordinate space. Comparing the HERWIG-generated D^*p distribution with the signal reported by H1, we determine the coalescence-enhancement factor $F_{\text{co}} \sim 10$. This is then applied to estimate the number of Θ_c events in e^+e^- annihilation at LEP and $p\bar{p}$ collisions at the Tevatron. For each of the four LEP experiments the model then predicts between 25 and 40 H1-like Θ_c events. For the Tevatron a signal of many thousands of events would have been expected.

Since both LEP and Tevatron experiments reported null results, our analysis implies that the either the H1 signal is spurious and due to an unknown systematic effect, or alternatively that it corresponds to a real resonance, whose production mechanism in DIS

is substantially different from the production mechanism in e^+e^- and the Tevatron. Yet another possibility is that either the theoretical or experimental analysis is missing an essential ingredient.

The value of $F_{co} \sim 10$ required to account for the H1 data is surprisingly large. In the event that further analysis of the data implies a smaller signal, or an upper limit, the value of F_{co} can be scaled down to obtain the correspondingly reduced predictions for e^+e^- and $p\bar{p}$. It should be noted that only the overall normalization of the predicted distributions and not their shapes will be affected by this procedure. As remarked in sect. 2.2, one possible effect that would lead to a reduced estimate of F_{co} is a higher proton yield in charm production in DIS, relative to the HERWIG prediction.

Acknowledgments

The research of one of us (M.K.) was supported in part by a visiting fellowship grant from the Royal Society and by the United States-Israel Binational Science Foundation (BSF), Jerusalem. We would like to thank Yeon Sei Chung, Karin Daum, Leonin Gladilin, Peter Hansen, Uri Karshon and Terry Sloan for useful discussions of the experimental data.

References

- [1] T. Nakano *et al.* [LEPS Coll.], Phys. Rev. Lett. **91**, 012002 (2003), hep-ex/0301020;
- [2] V. V. Barmin *et al.* [DIANA Coll.], Phys. Atom. Nucl. **66**, 1715 (2003) [Yad. Fiz. **66**, 1763 (2003)], hep-ex/0304040; S. Stepanyan *et al.* [CLAS Coll.], Phys. Rev. Lett. **91**, 252001 (2003), hep-ex/0307018; J. Barth *et al.* [SAPHIR Coll.], hep-ex/0307083; A. E. Asratyan, A. G. Dolgolenko and M. A. Kubantsev, hep-ex/0309042; V. Kubarovskiy *et al.* [CLAS Coll.], [Phys. Rev. Lett. **92**, 032001 (2004)] Erratum – ibid. **92**, 049902 (2004), hep-ex/0311046; R. Togoo *et al.*, Proc. Mongolian Acad. Sci., **4** (2003) 2; A. Airapetian *et al.* [HERMES Coll.], Phys. Lett. B **585**, 213 (2004) hep-ex/0312044; A. Aleev *et al.* [SVD Coll.], hep-ex/0401024; M. Abdel-Bary *et al.* [COSY-TOF Coll.], hep-ex/0403011; P. Z. Aslanyan, V. N. Emelyanenko and G. G. Rikhkvitzkaya, hep-ex/0403044; S. Chekanov *et al.* [ZEUS Coll.], hep-ex/0403051; T. Nakano, talk at NSTAR 2004, March 24-27, Grenoble, France, <http://lpsc.in2p3.fr/congres/nstar2004/talks/nakano.pdf> ; Y. A. Troyan *et al.*, hep-ex/0404003.
- [3] M. Karliner and H. J. Lipkin, hep-ph/0307343.
- [4] M. Karliner and H. J. Lipkin, hep-ph/0307243. M. Karliner and H.J. Lipkin, Phys. Lett. B **575** (2003) 249.
- [5] J. L. Rosner, Phys. Rev. D **69**, 094014 (2004), hep-ph/0312269.
- [6] T. E. Browder, I. R. Klebanov and D. R. Marlow, Phys. Lett. B **587**, 62 (2004), hep-ph/0401115.
- [7] S. Armstrong, B. Mellado and S. L. Wu, hep-ph/0312344.
- [8] A. Aktas *et al.* [H1 Collaboration], Phys. Lett. B **588**, 17 (2004), hep-ex/0403017.

- [9] L. Gladilin [on behalf of ZEUS Coll.], DESY seminar 12/3/04, <http://webcast.desy.de/Pentaquark120304.htm> ;
 U. Karshon [on behalf of ZEUS Coll.], talk at DIS 2004, Strbské Pleso, Slovakia, 14-18 April, <http://www.saske.sk/dis04/talks/D/karshon.ps.gz> ;
 ZEUS Coll., hep-ex/0409033.
- [10] “A Search for a State which Decays to a Charged D^* and Proton at FOCUS”, http://www-focus.fnal.gov/penta/penta_charm.html .
- [11] P. Hansen [for ALEPH Coll.], talk at DIS 2004, <http://www.saske.sk/dis04/talks/C/hansen.pdf> ;
 S. Schael *et al.*, [ALEPH Coll.], CERN-PH-EP-2004-038, to appear in Phys. Lett. B, <http://cdsweb.cern.ch/search.py?recid=789636> .
- [12] Yeon Sei Chung [for the CDF collaboration], Chicago Flavor Seminar, <http://b0urpc.fnal.gov/~yschung/Chicago-Flavor.pdf> .
- [13] G. Corcella *et al.*, JHEP **0101** (2001) 010 [arXiv:hep-ph/0011363].
- [14] G. Corcella *et al.*, arXiv:hep-ph/0210213.
- [15] T. Sjostrand and V. A. Khoze, Z. Phys. C **62** (1994) 281 [arXiv:hep-ph/9310242].
- [16] A. D. Martin, R. G. Roberts, W. J. Stirling and R. S. Thorne, Phys. Lett. B **443** (1998) 301 [arXiv:hep-ph/9808371].
- [17] A. Aktas *et al.* [H1 Collaboration], arXiv:hep-ex/0408149.
- [18] S. Chekanov *et al.* [ZEUS Collaboration], Phys. Rev. D **69** (2004) 012004 [arXiv:hep-ex/0308068];
 M. Wing, arXiv:hep-ex/0407049.
- [19] S. Eidelman *et al.*, Phys. Lett. **B592**, 1 (2004).
- [20] M. Karliner and H. J. Lipkin, arXiv:hep-ph/0405002.
- [21] A. Aktas *et al.* [H1 Collaboration], hep-ex/0403056.
- [22] I. G. Knowles and G. D. Lafferty, J. Phys. G **23**, 731 (1997) hep-ph/9705217.
- [23] G. Gustafson and J. Hakkinen, Z. Phys. C **61**, 683 (1994).
- [24] R. Akers *et al.* [OPAL Collaboration], Z. Phys. C **67**, 203 (1995).
- [25] T. Sloan, private communication.
- [26] P. J. Bussey, arXiv:hep-ex/0408020.